JOURNAL OF NEUROTRAUMA 34:182–191 (January 1, 2017)

DOI: 10.1089/neu.2015.4315

Diffusion-Derived Magnetic Resonance Imaging Measures of Longitudinal Microstructural Remodeling Induced by Marrow Stromal Cell Therapy after Traumatic Brain Injury

Lian Li,[1] Michael Chopp,[1,2] Guangliang Ding,[1] Changsheng Qu,[3] Siamak P. Nejad-Davarani,[1] Esmaeil Davoodi-Bojd,[1] Qingjiang Li,[1] Asim Mahmood,[3] and Quan Jiang[1,2]

Abstract

Using magnetic resonance imaging (MRI) and an animal model of traumatic brain injury (TBI), we investigated the capacity and sensitivity of diffusion-derived measures, fractional anisotropy (FA), and diffusion entropy, to longitudinally identify structural plasticity in the injured brain in response to the transplantation of human bone marrow stromal cells (hMSCs). Male Wistar rats (300–350g, $n=30$) were subjected to controlled cortical impact TBI. At 6 h or 1 week post-injury, these rats were intravenously injected with 1 mL of saline (at 6 h or 1 week, $n=5$/group) or with hMSCs in suspension ($\sim 3\times10^6$ hMSCs, at 6 h or 1 week, $n=10$/group). *In vivo* MRI measurements and sensorimotor function estimates were performed on all animals pre-injury, 1 day post-injury, and weekly for 3 weeks post-injury. Bielschowsky's silver and Luxol fast blue staining were used to reveal the axon and myelin status, respectively, with and without cell treatment after TBI. Based on image data and histological observation, regions of interest encompassing the structural alterations were made and the values of FA and entropy were monitored in these specific brain regions. Our data demonstrate that administration of hMSCs after TBI leads to enhanced white matter reorganization particularly along the boundary of contusional lesion, which can be identified by both FA and entropy. Compared with the therapy performed at 1 week post-TBI, cell intervention executed at 6 h expedites the brain remodeling process and results in an earlier functional recovery. Although FA and entropy present a similar capacity to dynamically detect the microstructural changes in the tissue regions with predominant orientation of fiber tracts, entropy exhibits a sensitivity superior to that of FA, in probing the structural alterations in the tissue areas with complex fiber patterns.

Keywords: diffusion; diffusion entropy; FA; MSCs; white matter reorganization

Introduction

Traumatic brain injury (TBI) remains a leading cause of neurological mortality and disability. An average of 1,400,000 TBIs occur each year in the United States, and >5,000,000 people are living with TBI-related disability at an annual cost of > $56,000,000,000.[1] TBI initiates multiple biochemical perturbations[2–4] that lead to secondary brain injury. Currently, no clinical treatment is available to repair the diffuse axonal injury, reverse the pathologic cascade of cell death, and reduce functional deficits following TBI.[5–7] However, recent investigations show that cell transplantation, which amplifies endogenous regenerative and restorative processes, has potential as a therapeutic strategy to attenuate devastating secondary pathological processes and meanwhile, to enhance brain plasticity.[8–10] As the key mechanism of damage, axonal injury is directly associated with neurobehavioral outcome,[11,12] whereas axonal remodeling, an adaptive brain response to trauma, which compensates for loss of function and could be promoted by cell engraftment,[13–15] has received increasing attention. These structural alterations within the injured brain can be revealed by magnetic resonance imaging (MRI), especially diffusion measurements.[16–21]

By exploiting the anisotropic properties of water diffusion in white matter (WM), diffusion imaging technology provides new insights into the microstructural organization of the central nervous system. As a noninvasive tool capable of characterizing the major diffusion direction of fiber tracts, diffusion-tensor imaging (DTI)[22] maps the orientational architecture of neural tissue *in vivo*. Fractional anisotropy (FA), one of the DTI-derived indices, describes

Departments of [1]Neurology and [3]Neurosurgery, Henry Ford Hospital, Detroit, Michigan.
[2]Department of Physics, Oakland University, Rochester, Michigan.

the degree of directionality of tissue water diffusion.[23] Because of its ability to capture the alteration of WM integrity, FA is widely used in experimental study[20,24,25] and clinical research[16,21,26] to quantify the extent of structural pathology or therapeutic benefit following brain insult. Although DTI holds value as an excellent imaging modality for identifying axonal injury as well as neuroplasticity that occur in the injured brain[18,27,28] it has a well-known inherent limitation, stemming from the constraints of the tensor model, which prevent DTI from adequately resolving intravoxel fiber crossing.[29] This significant shortcoming of DTI has motivated the introduction of alternative model-independent methods that directly use diffusion-weighted imaging for accurately characterizing anisotropic diffusion in complex neural tissue and for precisely detecting structural changes in response to injury and/or treatment. One of these novel proposed approaches is diffusion entropy,[30,31] which is based on information theory[32] and generated from the diffusion attenuation values measured across the applied diffusion-sensitizing gradient directions. Previous studies show that the entropy measure has advantages over FA by providing superior anisotropy-dependent image contrast and demonstrating increased sensitivity to axonal density.[30,31]

Cumulative evidence obtained from histological analysis, imaging investigation, and neuropsychological assessment supports the induction of brain structural plasticity provoked by injury,[33–36] which provides a biological substrate for spontaneous functional recovery. Promotion of such an ability of the brain to maximize repair capacity might, therefore, be a significant target for therapeutic strategies. This post-injury structural remodeling can be enhanced by proper treatment such as cell engraftment.[7,9,37–48] Cell transplantation after TBI promotes WM reorganization,[13–15] which can be detected by FA.[20] The advent of advanced model-free estimate MRI, such as diffusion entropy,[30,31] raises the exciting possibility that brain structural reorganization evoked by the therapeutic intervention could be revealed, which may add to our understanding of the role of structural remodeling as underlying functional recovery. However, quite limited data exist regarding the use of entropy to dynamically monitor structural changes, particularly for cell-induced neural remodeling in TBI. In addition, the timing of cell transplantation, one of key issues regarding optimization of basic transplantation techniques, remains to be addressed. Although acute intravenous cell intervention (within 24 h) after TBI provides therapeutic benefit above that of delayed cell administration ($\sim$1 week) in retarding cerebral atrophy and reducing functional deficits,[49,50] how these treatment strategies affect structural plasticity is unclear. The objective of the present study was to investigate the capacity and sensitivity of FA and entropy to: 1) longitudinally identify structural reorganization in an experimental animal model of TBI, and 2) dynamically detect the therapeutic effect of human bone marrow stromal cells (hMSCs), engrafted at 6 h or 1 week post-TBI, on structural remodeling in the injured brain. We tested the hypothesis that entropy, an information-based estimate without any model assumptions on the diffusion process, would be superior to FA in probing the structural alteration in response to the cell therapy after TBI, particularly in the tissue area with crossing fibers.

Methods

All experimental procedures were conducted in accordance with the National Institues of Health (NIH) Guide for the Care and Use of Laboratory Animals and approved by the Institutional Animal Care and Use Committee (IACUC) of Henry Ford Health System.

Animal model and experimental groups

The controlled cortical impact (CCI) TBI animal model employed has been previously described.[49,50] Briefly, male Wistar rats (300–350 g, $n=30$) were anesthetized with chloral hydrate (350 mg/kg, i.p.) and their rectal temperature was maintained at 37°C with a feedback-regulated water-heating pad. The head of each animal was mounted in a stereotactic frame and two 10 mm diameter craniotomies, one in each hemisphere, were performed adjacent to the central suture, midway between lambda and bregma, leaving the dura mater over the cortex intact. The left craniotomy confined the location of experimental impact whereas the right one allowed for the lateral movement of cortical tissue. Using a CCI device, a unilateral brain injury was induced by delivering a single impact at a velocity of 4 m/sec reaching a depth of 2.5 mm below the dura mater layer to the left cortex with a pneumatic piston containing a 6 mm diameter tip. Following the operation, the bone flap was replaced and sealed with bone wax, and the skin was sutured. For analgesia, Buprenex (0.05 mg/kg, s.q.) was administered to each animal after brain injury.

To investigate how cell therapy benefits structural remodeling and whether acute cell engraftment advances the therapeutic effect compared with delayed intervention, strategies previously proven efficient in improvement of neurological function, including cell type, dose, and treatment time point,[49,50] had been used.

MSCs are a mixed cell population, including stem and progenitor cells.[46] The hMSCs were provided by Theradigm (Baltimore, MD). The cells were suspended in phosphate-buffered saline (PBS) prior to injection into rats, which was performed at 6 h or 1 week post-TBI. Rats subjected to brain injury were randomized to one of four treatment groups, 6 h cell-treated ($n=10$), 1 week cell-treated ($n=10$), 6 h saline-treated ($n=5$), and 1 w saline-treated ($n=5$) groups. Anesthesia was reinstituted before the transplantation and a bolus of the cell suspension ($\sim 3\times10^6$ hMSCs in 1 mL PBS) was slowly infused over a 5 min period into the tail vein of each rat in the cell-treated groups using a Hamilton syringe. The needle was left in place for 1 min before withdrawal to minimize cell leakage, and the injection site was compressed for a short time to reduce bleeding. Replacing the cell suspension with the same amount of saline, each animal in the saline-treated groups underwent the identical procedure as those in the cell-treated groups.

Diffusion entropy

Diffusion anisotropy is a direct consequence of biological barriers and hindrances the water molecules experience as they passively diffuse. These diffusing molecules probe, on a microscopic scale, the underlying tissue structure.[31]

Shannon entropy provides a measure of uncertainty or randomness based on information theory. By applying Shannon entropy to investigate the diffusion-weighted data, it was hypothesized that tissue types with varying degrees of diffusion anisotropy could be differentiated based on their underlying information content, with a higher entropy or uncertainty reflecting a severer diffusion anisotropy. Diffusion entropy, E, was calculated pixel by pixel using the following formula:[19]

$$E(x_i) = -\sum_{d_j \in D} p(x_i, d_j) \log p(x_i, d_j)\ x_i \in FOV$$

where D is the set of all gradient directions in q-ball sequence, and $p(x_i,d_j)$ is the probability of the MRI signal attenuation value being repeated throughout D as a result of water displacement along a certain spatial orientation d_j for pixel x_i, and the MRI signal attenuation value for pixel x_i in diffusion direction d_j is calculated by dividing its diffusion-weighted signal intensity by pixel x_i's diffusion-free ($b=0$ sec/mm^2) signal intensity.

MRI and data processing

MRI was performed using ClinScan 7T system (Siemens, Erlanger, Germany). The animal was securely fixed on an MR-compatible holder equipped with a nose cone for administration of anesthetic gases and stereotaxic ear bars to immobilize the head. For reproducible positioning of the animal in the magnet, a fast gradient echo imaging sequence was used at the beginning of each MRI session. During image acquisition, anesthesia was maintained by a gas mixture of 1.0–1.5% isoflurane in medical air (1.0 L/min), and rectal temperature was kept at 37 ± 1.0°C using a feedback-controlled water bath (YSI Inc, Yellow Springs, OH) underneath the animal. T2-weighted imaging (T2WI) and DTI were acquired for all animals 1 day pre-TBI, 1 day post-TBI and then weekly for 3 weeks. All rats were killed after the final *in vivo* MRI scans.

T2WI was acquired using a multi-slice (13 slices, 1 mm thick), multi-echo (6 echoes) sequence with echo times (TE) of 15, 30, 45, 60, 75, and 90 ms and a repetition time (TR) of 4.5 sec. Images were produced with a 32×32 mm^2 field of view (FOV) and a 128×64 image matrix. Q-ball DTI was accomplished using a single-shot spin-echo echo-planer sequence with one baseline of $b = 0$ sec/mm^2 and 64 diffusion directional measurements at $b = 1500$ sec/mm^2 (32×32 mm^2 FOV, 128×128 image matrix, 13 slices (1 mm thick), TE = 50 ms, TR = 10 sec).

FA and entropy maps were generated using DTIstudio (Johns Hopkins University, Baltimore, MD) and an in-house software, respectively. Whereas T2 maps were calculated on a voxel-wise basis by linear least-squares fit of the logarithm of the signal intensity versus TE (Eigentool Image Analysis Software, Henry Ford Health System, MI), the orientation distribution function at each voxel was computed from q-ball imaging with Camino (Microstructure Imaging Group, University College London, London, UK).

Before quantification and analysis, the image distortion induced by eddy currents during diffusion measurement has to be rectified. For this task, an image registration software known as bUnwarpJ,[51] which was designed to align pairs of images distorted by both physical and acquisition-related distortions, was used. The approach combines the ideas of elastic and consistent image registration and minimizes the similarity error between the target and source image after imposing a consistency constraint. As a bidirectional registration, the algorithm calculates deformation fields for both direct (from source image to target image) and inverse (from target image to source image) transformation simultaneously. All slices of FA and entropy map (source image) were registered onto their corresponding slices of T2 map (target image), which served as reference for delineating the particularly targeted regions. Because the values of FA and entropy may change after registration procedure, the quantification was not performed on the registered image. Instead, the lesion and boundary regions of interest (ROIs) based on target image (T2 map) were inversely transformed to source image (original FA and entropy map) where the estimation was conducted.

As shown in Figure 1, cortical lesion was present on T2 as a hyperintensive area (arrow in Fig. 1A). Two distinct microstructural changes were revealed on both FA and entropy as a reduced lesion area with elevated boundary regions (red arrows in Fig. 1B and C). In these pericontusional cortex regions, WM reorganization was present after injury, which was confirmed by histological observation (Fig. 1D). To track the structural remodeling and compare the treatment effect (6 h cell or 1 week cell vs. saline) in this specific boundary region, the lesion was identified on a T2 map using a threshold value[49,50] provided by pre-injury scan. An ROI, encompassing the boundary region with apparent signal increase on FA and entropy map, was created by expanding the outline of the lesion 6 pixels outward in the cortex area (Fig. 1E, Eigentool). Values of FA and entropy were monitored in both the lesion and boundary region. For each animal, measurements were performed at observation time points post-TBI, and data were normalized to FA or entropy values of the homogeneous tissue areas provided by its pre-injury scan.

Modified neurological severity score

The modified neurological severity score (mNSS)[52] grades the composite neurological function of an animal on motor (muscle status and abnormal movement), sensory (visual, tactile, and proprioceptive), reflex and balance tests. One point is awarded for the inability of an animal to perform the tasks correctly or for the lack of a tested reflex (normal score: 0; maximal deficit score: 18). Therefore, the higher the score, the more severe the neurological dysfunction. mNSS was assessed for each animal 1 day pre-TBI, 1 and 4 days post-TBI, and weekly thereafter by an examiner blinded to the treatment groups and the corresponding MRI results.

Tissue preparation and histological evaluation

Immediately after the final *in vivo* MRI measurements at 3 weeks after TBI, rats were anesthetized intraperitoneally with 4% chloral hydrate, and perfused transcardially first with saline solution, followed by 4% paraformaldehyde in 0.1M PBS (pH 7.4). Their brains were removed, post-fixed in 4% paraformaldehyde at room temperature for 2 days, and then cut into seven standard coronal blocks (2 mm) on a rodent brain matrix. A series of adjacent sections (6 μm) was sliced with a microtome from each block embedded in paraffin and stained for histological evaluation.

To detect the axonal fiber tracts, a double staining, Bielshowsky's silver and Luxol fast blue (B+LFB) staining, was performed to demonstrate axons and myelin, respectively. For Bielshowsky's silver staining, sections were first incubated in 20% silver nitrate in the dark, followed by adding ammonium hydroxide until the tissues turned brown with a gold background. The sections were then treated with sodium thiosulfate. Finally, sections were stained in Luxol fast blue solution, washed in 95% alcohol, and placed in lithium carbonate. Under a light microscope, myelin appears as blue whereas axons are black on the stained tissue slice.

For axon quantification, the density of the immunoreactive area along the lesion boundary zone was measured under the microscope using 20× objective. Data were collected in the pericontusional cortex regions (as indicated in Fig. 1E) from six fields (three fields per side)[49] and presented as the average percentage of positive area.

Statistical analysis

Statistical analysis was performed using SAS (Cary, NC, version 9.2). Analysis of covariance (ANCOVA) was employed to compare the group difference in MRI measurements (lesion volume, FA, and entropy) and functional assessments (mNSS) with the independent factor of treatment and dependent factor of time. The treatment effect on mNSS was conducted based on the ranked data, because the data were not normally distributed. Analysis began with testing the treatment group and time interaction, followed by testing the group difference at each time point and the time effect for each treatment group if the interaction or the overall group/time effect was detected at the 0.05 level. A subgroup analysis would be considered if the interaction or main effect of group/time was not at the 0.05 level. Density of the immunoreactive area was analyzed by two sample t test. Results are presented as mean ± standard error (SE). Statistical significance was inferred for $p \leq 0.05$.

Results

All animals with saline injection post-TBI were considered as a saline-treated group, becaue no tendency towards statistical differences in MRI measurements, histological estimates, and functional

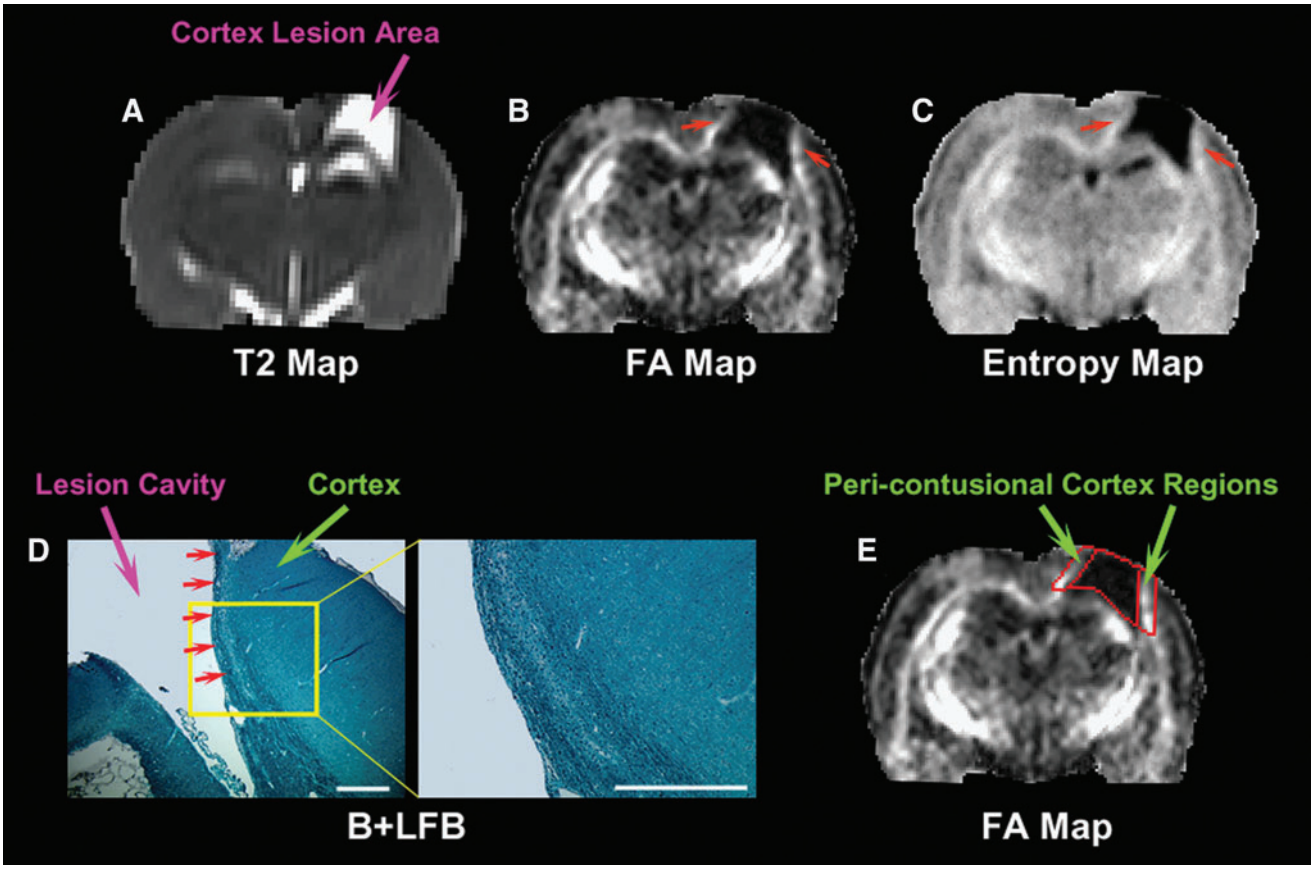

FIG. 1. Representative section of a 6 h cell-treated animal (3 weeks post-traumatic brain injury [TBI]) showing white matter (WM) reorganization and region of interest (ROI) creation. Cortex lesion exhibits hyperintensive area on T2 map **(A)**, which corresponds to the hypointensive area on the fractional anisotropy (FA) map **(B)**, indicative of structural disruption. The hyperintensities on the FA map are detected in the cortex regions near the lesion (red arrows in **B**). A similar pattern is present on the entropy map (red arrows in **C**). Bielshowsky's silver and Luxol fast blue (B+LFB) stain (**D**, scale bars = 500 μm) reveals that these pericontusional cortex regions contain oriented and extended bundles of axons, suggesting WM reorganization. Whereas T2 hyperintensities identify the lesion area **(A)**, the 6 pixel wide ROIs immediately adjacent to the lesion encompass the lesion boundary regions with structural remodeling **(E)**.

outcomes between the 6 h saline-treated and the 1 week saline-treated groups were found.

White matter reorganization detected by FA and entropy

The abnormal hyperintensities on the T2 map (indicated by arrow in Fig. 1A) represent the affected injured cortical tissue after TBI, whereas abnormal values on the FA map reflect the structural alteration, with hypointensities indicating tissue structural disruption, and hyperintensities denoting the increased intensity or directionality of fiber tracts.

In contrast to the lesion area with decreased FA value, our image data revealed a specific territory with elevated FA value following brain injury. As visualized on the FA map (red arrows in Fig. 1B), notable hyperintensities appeared in the adjacent boundary regions. The hyperintensities appeared to extrude from the relatively intact structure and develop along the lesion boundary. A similar pattern of hyperintensive boundary regions was also present on the entropy map (red arrows in Fig. 1C). As shown by B+LFB stain (Fig. 1D), the oriented bundles of myelinated axons extending from the normal-appearing area with dense tracts were present in these pericontusional cortex regions, signifying WM reorganization. This structural remodeling occurs after TBI with or without cell treatment, and importantly, both FA and entropy are sensitive to this axonal remodeling.

Dynamic changes of microstructure detected by FA and entropy

As illustrated by sets of T2 and FA maps, typical examples of longitudinal structural reorganization along the boundary region with and without cell transplantation after TBI are provided in Figure 2. Because the FA and entropy map exhibit a similar pattern for this post-injury structural remodeling (compare Fig. 1B with 1C), only the FA maps that matched the T2 maps were provided here for clarity of presentation. Compared with the saline-treated animals, hyperintensive regions near the lesion on the FA map (arrows in Fig. 2), starting from 2 weeks after TBI, were evident in the cell-treated animals, representing the enhanced structural reorganization in response to the cell therapy. Moreover, the bright regions were wider and denser in the 6 h cell-treated animal than in the 1week cell-treated animal (compare Fig. 2E, F with Fig. 2K, L), suggesting a stronger therapeutic effect after an acute cell intervention than after a delayed cell administration. This microstructural remodeling process, however, was less evident for the

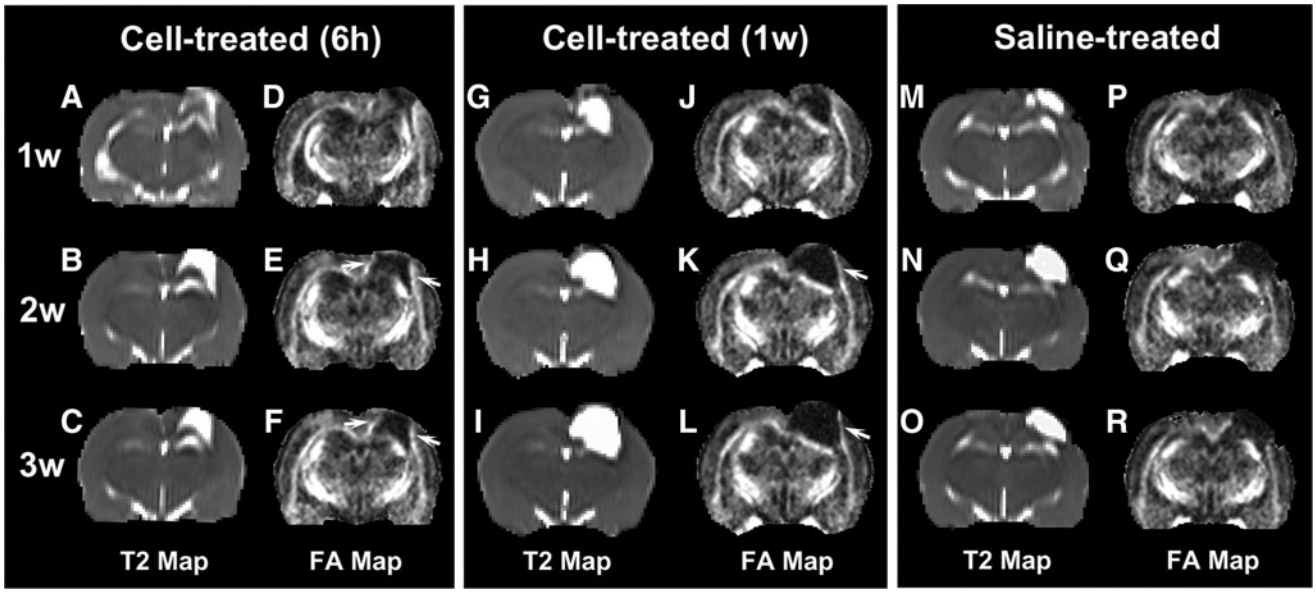

FIG. 2. Sets of T2 (**A–C, G–I, M–O**) and fractional anisotropy (FA) (**D–F, J–L, P–R**) maps longitudinally illustrating the structural remodeling with and without cell intervention after traumatic brain injury (TBI). Cell administration executed either at 6 h or 1 week post-TBI enhances white matter (WM) reorganization, as shown by the hyperintensities developing along the lesion boundary (arrows in **E, F** and **K, L**). A stronger therapeutic effect, indicated by the presence of wider and denser hyperintensive areas in the boundary regions on FA map, is found in the 6 h cell-treated animal than in the 1 week cell-treated animal (compare **E, F** with **K, L** in the lesion boundary regions). This microstructural remodeling progression, however, is less evident for the saline-treated animals (compare **Q, R** with **E, F** and **K, L** in the lesion boundary regions).

saline-treated animals (compare Fig. 2Q, R with Fig. 2E, F and Fig. 2K, L in the lesion boundary regions).

Using the same width ROI (Fig. 1E), quantification for FA and entropy was performed in the boundary region (Fig. 3). For comparison, estimates of FA and entropy were also conducted in the lesion area. Related to the pre-injury status, increased FA and entropy values were evident in the boundary region post-injury (relative values >1), whereas decreased values were present in the lesion area (relative values <1) as expected for all groups. At 2 weeks after TBI (Fig. 3A, B), no significant differences among three treatment groups were found for either FA or entropy values either in the lesion or in the boundary area, although the mean values of FA and entropy in the boundary area were higher in the cell-treated groups than in the saline-treated group. At 3 weeks after TBI (Fig. 3C, D); however, significantly increased FA and entropy were detected in the boundary area only in the 6 h cell-treated animals compared with the controls.

Sensitivity of FA and entropy to structural alterations

Our imaging data indicate that entropy provides more information regarding dynamic structural alterations than does FA, particularly in the tissue area with crossing fibers. A representative example of a 6 h cell-treated animal is given in Figure 4. At 1 day after TBI, both FA and entropy detect the hypointensive area in the cortex region, corresponding to the hyperintense lesion identified on T2 (compare Fig. 4A with 4B and C). From 1 day to 2 weeks post-TBI, entropy reveals the evolution of tissue structural status (compare Fig. 4F with 4C), which nicely matches the apparent change of the hyperintense T2 lesion in both size and shape (compare Fig. 4D with 4A). The restored tissue region captured on entropy (red arrow in Fig. 4F) corresponds to the recovery area from hyperintensities on T2 (compare Fig. 4D with 4F). This structural alteration, however, is not reflected on FA (compare Fig. 4E with 4B). The fiber orientation map (Fig. 4G) shows that the tissue area present on entropy (red arrow in Fig. 4F), but absent on FA (Fig. 4E), primarily contains crossing fibers.

Focal lesion, histological and functional outcome

Administration of hMSCs either at 6 h or 1 week after TBI does not reduce the focal lesion volume (Fig. 5A), but results in increased axonal remodeling and improved functional outcome (Fig. 5B, C), with acute cell intervention (6 h) leading to a higher axonal density along the lesion boundary (Fig. 5B) and an earlier functional recovery (Fig. 5C) than delayed cell transplantation (1 week).

Discussion

With MRI and an experimental animal model of TBI, the capacity and sensitivity of diffusion-derived measures, FA, and entropy, to longitudinally identify structural plasticity in the injured brain, especially the structural changes in response to the transplantation of hMSCs, were investigated *in vivo*. Our data show that adaptive structural remodeling without treatment after TBI as well as hMSC-enhanced structural reorganization along the lesion boundary zone can be revealed by both FA and entropy MRI. Compared with delayed cell administration (1 week), acute cell intervention (6 h) after TBI promotes this brain restorative process, which occurs in parallel with an earlier functional improvement. We demonstrate the superiority of entropy over FA in dynamically probing the structural alterations, particularly in the tissue area with complex fiber patterns.

FA has been widely used to quantify the anisotropic property of water diffusion in the brain, with a higher FA value indicating

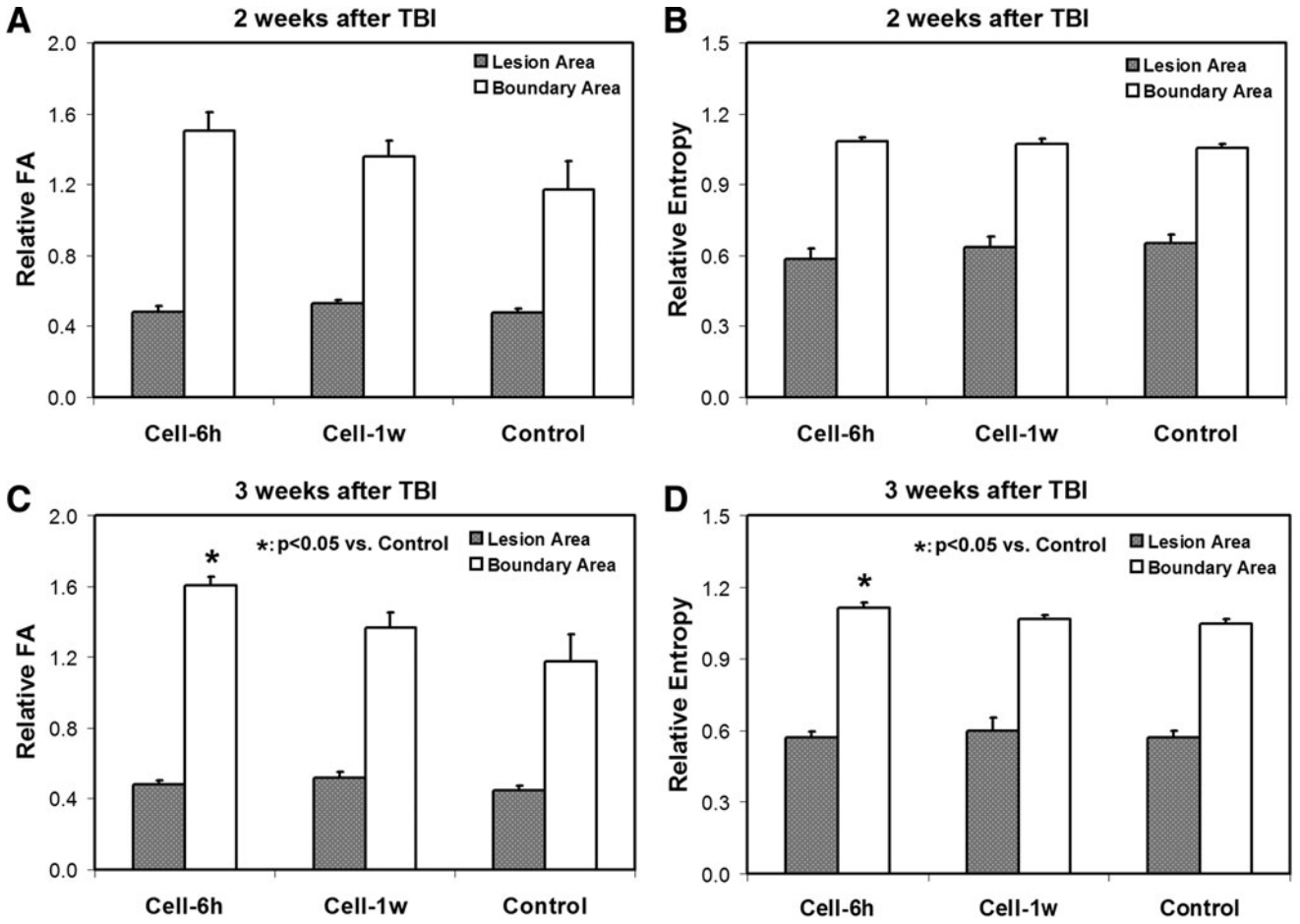

FIG. 3. Changes of fractional anisotropy (FA) (**A, C**) and entropy (**B, D**) values in the lesion and boundary areas. At 2 weeks after traumatic brain injury (TBI) (**A, B**), no statistical differences among the three treatment groups are found for either FA or entropy values either in the lesion or in the boundary area. At 3 weeks after TBI (**C, D**), however, significant increased FA and entropy are detected in the boundary area only in the 6 h cell-treated animals compared with the controls.

higher density and greater directionality of myelinated fiber tracts.[20,24,26,53–55] As an alternative approach, entropy provides a measure of anisotropy of diffusion based on information theory.[31,32] Without restriction, diffusion of water molecules is isotropic. In this situation, diffusion attenuation of MRI signal is independent of gradient directions, giving the lowest entropy or the lowest anisotropy of diffusion. This, however, is not the case with brain tissue that contains complex structure that restricts water molecular diffusion. In this situation, diffusion attenuation is then highly dependent on gradient directions, yielding higher entropy or higher anisotropy of diffusion. Changes of these diffusion-derived parameters (FA and entropy) in the neural tissue may, therefore, reflect axonal structural alteration.

Previous studies demonstrate that even without treatment intervention, axonal remodeling after TBI occurs in the injured brain, and such structural plasticity accounts for some of the functional improvements.[14,20,26,56,57] In agreement with these findings, our dynamic image data showed that FA in particular brain areas spontaneously increased after TBI, which was accompanied with an improvement of functional recovery as measured by mNSS. In addition, similarly to some sites in the brain that are particularly vulnerable to diffuse axonal injury following TBI,[27,58] there seem to be brain regions that are more prone to structural remodeling. For the animal model with severe TBI in the current study, an apparent structural reorganization following the injury is found in the lesion boundary regions, as revealed by both histological and imaging investigations.[14,20,24] In order to compare the capacity of FA and entropy to identify this structural alteration, we therefore focused specifically on the lesion boundary region.

The B+LFB stain showed the presence of oriented bundles of axons, adjacent to the lesion, which developed as a result of WM reorganization after TBI (Fig. 1D). Correspondingly, the area of WM remodeling with increased axonal anisotropy was evident on FA and entropy MRI as elevated pixels along the lesion boundary (red arrows in Fig. 1B and C), identifying the neural tissue with increased density of oriented fiber tracts. Also, the temporal profiles of this evolving fiber reorientation were captured by serial image data (Fig. 2). Quantitative monitoring and statistical analysis are necessary to demonstrate how FA and entropy characterize structural remodeling in the injured brain. For this purpose, the ROIs exclusively encompassing these boundary remodeling regions were identified (Fig. 1E) and the FA and entropy estimates were normalized to the values obtained from the pre-injury brain. As demonstrated in Figure 3, similar temporal patterns were found from FA and entropy measurements, which longitudinally represent the progression of structural remodeling in the boundary region. The FA and entropy values increased in each cell treatment group from 2 weeks to 3 weeks after TBI compared with the saline-

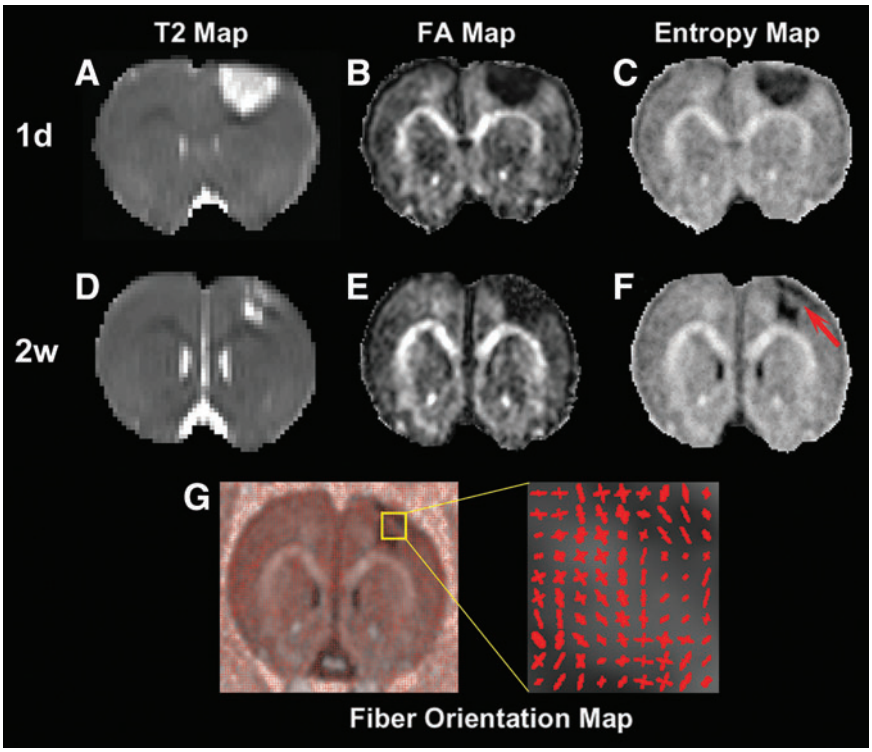

FIG. 4. A slice of a 6 h cell-treated animal longitudinally showing the sensitivity of fractional anisotropy (FA) and entropy to structural restoration. At 1 day after traumatic brain injury (TBI) (**A–C**), both FA **(B)** and entropy **(C)** detect the hypointensive area in the cortex region, which corresponds to the hyperintensive lesion identified on T2 **(A)**. From 1 day to 2 weeks after TBI (**D–F**), entropy reveals the dramatic evolution of structural status (compare **F** with **C**), which nicely matches the apparent change of T2 lesion (compare **D** with **A**) in both size and shape, with restored tissue region captured on entropy (red arrow in **F**) corresponding to recovery area from hyperintensities on T2 (compare **D** with **F**). This structural restoration, however, is not reflected on FA (compare **E** with **B**). The tissue recovery area present on entropy (red arrow in **F**), but absent on FA, mainly contains crossing fibers, as shown by fiber orientation map **(G)**.

treated group at each time point. Moreover, a significant treatment effect was detected by both FA and entropy at 3 weeks in the 6 h cell-treated animals compared with the controls, consistent with our histological evaluation (Fig. 5B). These data demonstrate that FA and entropy have a similar capacity to reveal the dynamics of reorganizing fiber tracts after TBI in the lesion boundary. *In vivo* quantification and statistical analysis collectively indicate that both FA and entropy were able to identify WM reorganization resulting from adaptive brain response to trauma without treatment, and to discern a subtle distinction between treatment strategies of transplantation of hMSCs at 6 h and 1 week on this structural change. Compared with delayed; (1 week), cell administration, acute cell intervention (6h) provided an advanced therapeutic benefit by expediting such restorative process (Fig. 3C, D), which may contribute in part to the corresponding earlier improvement of functional outcome (Fig. 5C).

In addition to the perilesional area with post-TBI reorientation of fiber tracts, our data showed that tissue structural remodeling also involves crossing fibers (Fig. 4). In this situation, however, entropy provided higher sensitivity than FA in dynamically probing the crossover fiber remodeling. As illustrated by a representative 6 h cell-treated animal (Fig. 4), lesion shrinkage from 1 day to 2 weeks was evident on T2 (compare Fig. 4A with 4D) because of the fading or returning toward normal of hyperintense pixels, implying tissue recovery.[20,59] Meanwhile, a dramatic evolution of tissue status with time was revealed by entropy (compare Fig. 4F with 4C), which matched the apparent change of hyperintensive T2 lesion in both size and shape during the same time span (compare Fig. 4D with 4A), with restored tissue region captured on entropy (red arrow in Fig. 4F) corresponding to recovery area from hyperintensities on T2 (compare Fig. 4D with 4F). This entropy-detected tissue structural restoration, supported by T2 measurements, however, was not reflected on FA (compare Fig. 4E with 4B). The different sensitivities between FA and entropy to this structural change may be attributed to the fact that the recovery area contained crossing fibers, and thereby reduced directional coherence of fiber arrangement (Fig. 4G), where FA encountered its significant inherent obstacle,[29] whereas entropy exhibited its advantage as a model-independent estimate.

As described previously,[14,50] our TBI model induced severe brain injury, which affected both the cortical and underlying subcortical regions. Damage to the corpus callosum, the principal and largest bundle of nerve fibers in the brain, and its reorganization afterwards, led to readily detected MRI signal change (Fig. 1). As evidenced by both our image and histological data, this robust structural plasticity occurring in the injured brain was found in all experimental groups and was enhanced in response to the engraftment of hMSCs (Figs. 2 and 3). The location of this major structural alteration within the narrow lesion boundary region made MRI and histological quantification feasible. Hence, this territory undergoing structural reorganization after TBI provided an ideal site to examine the evolution of FA and entropy indices in detecting neural fiber remodeling. Our image data and quantitative measurements demonstrate that the development of this restorative

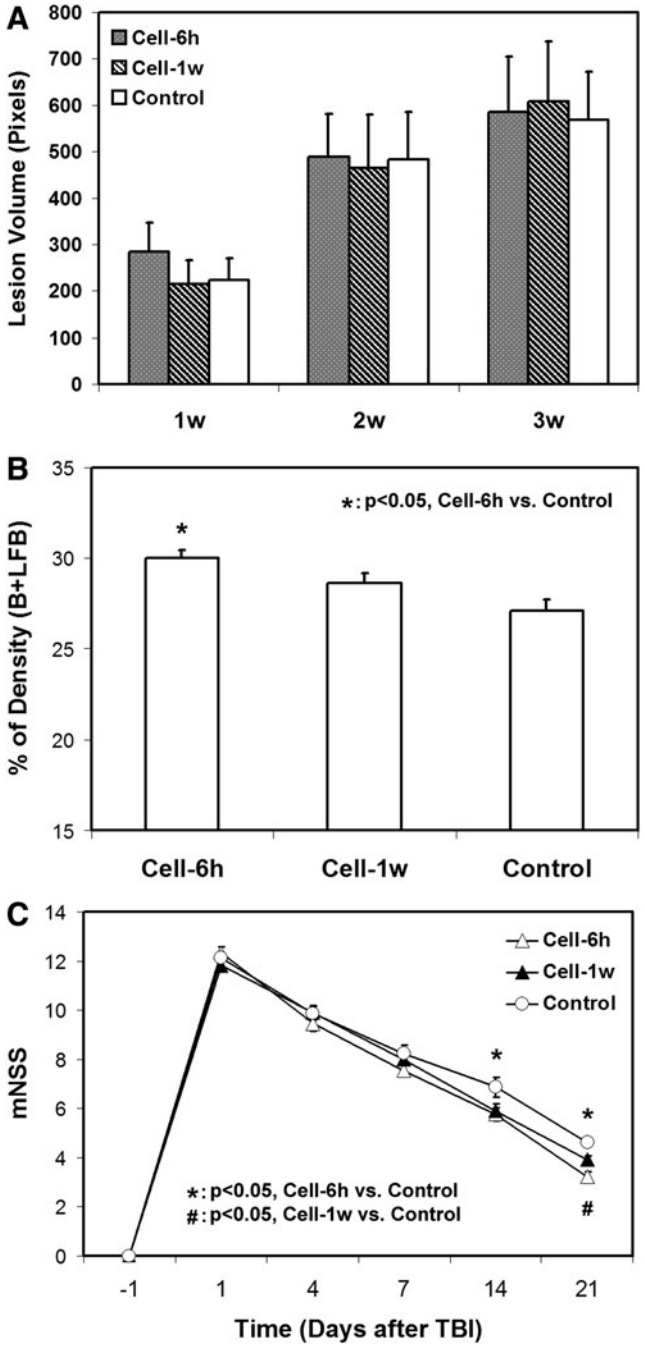

FIG. 5. Lesion volume and histological and functional outcome. Administration of human bone marrow stromal cells (hMSCs) either at 6 h or 1 week after TBI does not reduce the focal lesion volume **(A)**, but results in an increased axonal density in the lesion boundary zone, with significantly higher density being detected in the 6 h cell-treated group than in the control group **(B)**. Significantly improved functional performance, as measured by mNSS, is found in the cell-treated animals compared with the controls **(C)**. The effect starts at an earlier time point in the 6 h cell-treated animals (1–2 weeks) than in the 1 week cell-treated animals (2–3 weeks).

structural change can be depicted dynamically by both FA and entropy. Instead of a single unique location, however, ameliorative structural change occurs in multiple sites in the brain after TBI.[9,26,60] Supporting this multi-site cerebral remodeling post-TBI, our data demonstrate that entropy, not FA, identifies structural plasticity within tissue regions with crossing fibers (Fig. 4), in addition to the narrow boundary region consisting of highly parallel fibers (Fig. 1). This restored tissue region (red arrow in Fig. 4F) at an early stage of structural reorganization[30] was only observed in the 6 h cell-treated group within our experimental time frame, suggesting that acute cell intervention advanced the process of structural restoration compared with delayed cell transplantation. Our imaging data indicate that entropy, an information-based estimate without any model assumptions on the diffusion process, is superior to FA in longitudinally capturing the tissue structural alteration, especially from a complex structure with axonal crossover. Although previous investigators found that entropy had advantages over FA, they drew this conclusion based on cross-sectional data comparison.[30 31] Confirming and complementing these studies, the present study furnishes dynamic results, which provides information, particularly regarding the progression of complex multi-directional axonal remodeling in the traumatized brain, and offers insight into its role in underlying functional recovery with time.

Engrafted MSCs in the injured brain exert therapeutic effects via multiple mechanisms, such as increasing angiogenesis,[49,61] enhancing neurogenesis,[62] attenuating hypoperfusion,[49] upregulating neurotrophic growth factors,[41,63] suppressing growth-inhibitory molecules,[13,14,64] and reducing apoptosis.[65] All of these actions, likely in concert, contribute to a neurorestorative microenvironment within the brain, thereby promoting endogenous plasticity, facilitating axonal regeneration, and improving neurological outcome after TBI. With regard to the timing of cell transplantation, engraftment performed ≥1 day after TBI is widely selected to avoid the intense inflammatory and pathological metabolic response of the trauma-injured brain, which creates a milieu inhospitable for cell survival.[66] However, delayed engraftment experiences other conditions, including gliotic changes, which may negatively affect the efficacy of cell therapy.[6] Our previous studies[49,50] show that acute intravenous cell transplantation (e.g., 6 h) after TBI results in a greater therapeutic efficacy than delayed cell administration (e.g., 1 week) in preserving cerebral tissue and enhancing neurological functions. Herein, we further demonstrate that acute 6 h cell intervention also provides increased therapeutic benefit in structural restoration, likely because of both the neuroprotective and neurorestorative function of MSCs.[49,67]

The findings gained from the current study are meaningful and applicable to the clinic. As a diffusion-derived index with a high sensitivity particularly to complex structural change, diffusion entropy can be easily introduced into the clinical MRI, and the additional information gleaned from employing this imaging method may provide insight into the biological substrate underlying functional recovery. Cell transplantation, a promising therapy after brain injury, has a wide intervention window,[49,50] and acute intravenous cell administration after TBI may be a feasible choice when designing a clinical trial.

Conclusion

In summary, intravenous administration of hMSCs after TBI leads to WM reorganization, particularly along the boundary of the contusional lesion which can be identified by both FA and entropy. Compared to the hMSC therapy initiated at 1 week post-TBI, cell intervention initiated at 6 h increases brain remodeling, which may contribute in part to the corresponding earlier functional recovery found with the 6 h treatment. Whereas FA and entropy show similar capacity to dynamically detect the axonal structural changes in the

tissue region with dominant orientation of fiber tracts, entropy exhibits sensitivity superior to FA, in revealing the neural fiber structural alterations, particularly in areas with complex fiber patterns.

Acknowledgments

This work was supported by National Institutes of Health RO1 NS064134.

Author Disclosure Statement

No competing financial interests exist.

References

1. Langlois, J.A., Rutland-Brown, W., and Wald, M.M. (2006). The epidemiology and mpact of traumatic brain injury: a brief overview. J. Head Trauma Rehabil. 21, 375–378.
2. Stoica, B.A., and Faden, A.I. (2010). Cell death mechanisms and modulation in traumatic brain injury. Neurotherapeutics 7, 3–12.
3. Xu, Y., McArthur, D.L., Alger, J.R., Etchepare, M., Hovda, D.A., Glenn, T.C., Huang, S., Dinov, I., and Vespa, P.M. (2010). Early nonischemic oxidative metabolic dysfunction leads to chronic brain atrophy in traumatic brain injury. J. Cereb. Blood Flow Metab. 30, 883–894.
4. Ziebell, J.M., and Morganti–Kossmann, M.C. (2010). Involvement of pro- and anti-inflammatory cytokines and chemokines in the pathophysiology of traumatic brain injury. Neurotherapeutics 7, 22–30.
5. Parr, A.M., Tator, C.H., and Keating, A. (2007). Bone marrow-derived mesenchymal stromal cells for the repair of central nervous system injury. Bone Marrow Transplant. 40, 609–619.
6. Sharma, A., Sane, H., Kulkarni, P., Yadav, J., Gokulchandran, N., Biju, H., and Badhe, P. (2015). Cell therapy attempted as a novel approach for chronic traumatic brain injury – a pilot study. SpringerPlus 4, 26.
7. Xiong, Y., Zhang, Y., Mahmood, A., and Chopp, M. (2015). Investigational agents for treatment of traumatic brain injury. Exp. Opin. Investig. Drugs 24, 743–760.
8. Opydo–Chanek, M. (2007). Bone marrow stromal cells in traumatic brain injury (TBI) therapy: true perspective or false hope? Acta Neurobiol. Exp. 67, 187–195.
9. Xiong, Y., Mahmood, A., and Chopp, M. (2010). Neurorestorative treatments for traumatic brain injury. Discov. Med. 10, 434–442.
10. Xiong, Y., Mahmood, A., and Chopp, M. (2010). Angiogenesis, neurogenesis and brain recovery of function following injury. Curr. Opin. Investig. Drugs 11, 298–308.
11. Haberg, A.K., Olsen, A., Moen, K.G., Schirmer–Mikalsen, K., Visser, E., Finnanger, T.G., Evensen, K.A., Skandsen, T., Vik, A., and Eikenes, L. (2015). White matter microstructure in chronic moderate-to-severe traumatic brain injury: impact of acute-phase injury-related variables and associations with outcome measures. J. Neurosci. Res. 93, 1109–1126.
12. Hylin, M.J., Orsi, S.A., Zhao, J., Bockhorst, K., Perez, A., Moore, A.N., and Dash, P.K. (2013). Behavioral and histopathological alterations resulting from mild fluid percussion injury. J. Neurotrauma 30, 702–715.
13. Mahmood, A., Wu, H., Qu, C., Mahmood, S., Xiong, Y., Kaplan, D., and Chopp, M. (2014). Down-regulation of Nogo-A by collagen scaffolds impregnated with bone marrow stromal cell treatment after traumatic brain injury promotes axonal regeneration in rats. Brain Res. 1542, 41–48.
14. Mahmood, A., Wu, H., Qu, C., Mahmood, S., Xiong, Y., Kaplan, D.L., and Chopp, M. (2014). Suppression of neurocan and enhancement of axonal density in rats after treatment of traumatic brain injury with scaffolds impregnated with bone marrow stromal cells. J. Neurosurg. 120, 1147–1155.
15. Wang, E., Gao, J., Yang, Q., Parsley, M.O., Dunn, T.J., Zhang, L., DeWitt, D.S., Denner, L., Prough, D.S., and Wu, P. (2012). Molecular mechanisms underlying effects of neural stem cells against traumatic axonal injury. J. Neurotrauma 29, 295–312.
16. Bazarian, J.J., Zhong, J., Blyth, B., Zhu, T., Kavcic, V., and Peterson, D. (2007). Diffusion tensor imaging detects clinically important axonal damage after mild traumatic brain injury: a pilot study. J. Neurotrauma 24, 1447–1459.
17. Bendlin, B.B., Ries, M.L., Lazar, M., Alexander, A.L., Dempsey, R.J., Rowley, H.A., Sherman, J.E., and Johnson, S.C. (2008). Longitudinal changes in patients with traumatic brain injury assessed with diffusion-tensor and volumetric imaging. NeuroImage 42, 503–514.
18. Bosnell, R., Giorgio, A., and Johansen–Berg, H. (2008). Imaging white matter diffusion changes with development and recovery from brain injury. Dev. Neurorehabil. 11, 174–186.
19. Ding, G., Chen, J., Chopp, M., Li, L., Yan, T., Davoodi–Bojd, E., Li, Q., Davarani, S.P., and Jiang, Q. (2015). White matter changes after stroke in type 2 diabetic rats measured by diffusion magnetic resonance imaging. J. Cereb. Blood Flow Metab. (In press.)
20. Jiang, Q., Qu, C., Chopp, M., Ding, G.L., Davarani, S.P., Helpern, J.A., Jensen, J.H., Zhang, Z.G., Li, L., Lu, M., Kaplan, D., Hu, J., Shen, Y., Kou, Z., Li, Q., Wang, S., and Mahmood, A. (2011). MRI evaluation of axonal reorganization after bone marrow stromal cell treatment of traumatic brain injury. NMR Biomed. 24, 1119–1128.
21. Sidaros, A., Engberg, A.W., Sidaros, K., Liptrot, M.G., Herning, M., Petersen, P., Paulson, O.B., Jernigan, T.L., and Rostrup, E. (2008). Diffusion tensor imaging during recovery from severe traumatic brain injury and relation to clinical outcome: a longitudinal study. Brain 131, 559–572.
22. Basser, P.J., Mattiello, J., and LeBihan, D. (1994). Estimation of the effective self-diffusion tensor from the NMR spin echo. J Magn. Reson. B 103, 247–254.
23. Pierpaoli, C., and Basser, P.J. (1996). Toward a quantitative assessment of diffusion anisotropy. Magn. Reson. Med. 36, 893–906.
24. Ding, G.L., Chopp, M., Poulsen, D.J., Li, L., Qu, C., Li, Q., Nejad–Davarani, S.P., Budaj, J.S., Wu, H., Mahmood, A., and Jiang, Q. (2013). MRI of neuronal recovery after low-dose methamphetamine treatment of traumatic brain injury in rats. PloS One 8, e61241.
25. Xu, S., Zhuo, J., Racz, J., Shi, D., Roys, S., Fiskum, G., and Gullapalli, R. (2011). Early microstructural and metabolic changes following controlled cortical impact injury in rat: a magnetic resonance imaging and spectroscopy study. J. Neurotrauma 28, 2091–2102.
26. Farbota, K.D., Bendlin, B.B., Alexander, A.L., Rowley, H.A., Dempsey, R.J., and Johnson, S.C. (2012). Longitudinal diffusion tensor imaging and neuropsychological correlates in traumatic brain injury patients. Front. Hum. Neurosci. 6, 160.
27. Irimia, A., Wang, B., Aylward, S.R., Prastawa, M.W., Pace, D.F., Gerig, G., Hovda, D.A., Kikinis, R., Vespa, P.M., and Van Horn, J.D. (2012). Neuroimaging of structural pathology and connectomics in traumatic brain injury: Toward personalized outcome prediction. NeuroImage Clin. 1, 1–17.
28. Lerner, A., Mogensen, M.A., Kim, P.E., Shiroishi, M.S., Hwang, D.H., and Law, M. (2014). Clinical applications of diffusion tensor imaging. World Neurosurg. 82, 96–109.
29. Tuch, D.S. (2004). Q-ball imaging. Magn. Reson. Med. 52, 1358–1372.
30. Fozouni, N., Chopp, M., Nejad–Davarani, S.P., Zhang, Z.G., Lehman, N.L., Gu, S., Ueno, Y., Lu, M., Ding, G., Li, L., Hu, J., Bagher–Ebadian, H., Hearshen, D., and Jiang, Q. (2013). Characterizing brain structures and remodeling after TBI based on information content, diffusion entropy. PloS One 8, e76343.
31. Metwalli, N.S., LaConte, S.M., and Hu, X.P. (2006). An information theoretic approach characterizing diffusion anisotropy in diffusion-weighted magnetic resonance images. Presented at the Annual International Conference of the IEEE Engineering in Medicine and Biology Society 1, 2260–2263. New York, NY.
32. Shannon, C.E. (1997). The mathematical theory of communication. 1963. MD Comput. 14, 306–317.
33. Johansen–Berg, H. (2007). Structural plasticity: rewiring the brain. Curr. Biol. 17, R141–144.
34. Perederiy, J.V., and Westbrook, G.L. (2013). Structural plasticity in the dentate gyrus- revisiting a classic injury model. Front Neural Circuits 7, 17.
35. Dijkhuizen, R.M., van der Marel, K., Otte, W.M., Hoff, E.I., van der Zijden, J.P., van der Toorn, A., and van Meer, M.P. (2012). Functional MRI and diffusion tensor imaging of brain reorganization after experimental stroke. Transl. Stroke Res. 3, 36–43.
36. van der Zijden, J.P., Bouts, M.J., Wu, O., Roeling, T.A., Bleys, R.L., van der Toorn, A., and Dijkhuizen, R.M. (2008). Manganese-enhanced MRI of brain plasticity in relation to functional recovery after experimental stroke. J. Cereb. Blood Flow Metab 28, 832–840.

37. Chopp, M., Li, Y., and Zhang, Z.G. (2009). Mechanisms underlying improved recovery of neurological function after stroke in the rodent after treatment with neurorestorative cell-based therapies. Stroke 40, S143–145.
38. Gutierrez–Fernandez, M., Rodriguez–Frutos, B., Ramos–Cejudo, J., Otero–Ortega, L., Fuentes, B., and Diez–Tejedor, E. (2013). Stem cells for brain repair and recovery after stroke. Exp. Opin. Biol. Ther. 13, 1479–1483.
39. Aertker, B.M., Bedi, S., and Cox, C.S., Jr. (2016). Strategies for CNS repair following TBI. Exp. Neurol. 275, 411–426.
40. Peterson, D.A. (2002). Stem cells in brain plasticity and repair. Curr. Opin. Pharmacol. 2, 34–42.
41. Li, Y., Chen, J., Chen, X.G., Wang, L., Gautam, S.C., Xu, Y.X., Katakowski, M., Zhang, L.J., Lu, M., Janakiraman, N., and Chopp, M. (2002). Human marrow stromal cell therapy for stroke in rat: neurotrophins and functional recovery. Neurology 59, 514–523.
42. Li, Y., Chen, J., and Chopp, M. (2001). Adult bone marrow transplantation after stroke in adult rats. Cell Transplant. 10, 31–40.
43. Chopp, M., and Li, Y. (2002). Treatment of neural injury with marrow stromal cells. Lancet Neurol. 1, 92–100.
44. Chopp, M., Li, Y., and Zhang, J. (2008). Plasticity and remodeling of brain. J. Neurol. Sci. 265, 97–101.
45. Chen, J., and Chopp, M. (2006). Neurorestorative treatment of stroke: cell and pharmacological approaches. NeuroRx 3, 466–473.
46. Li, Y., and Chopp, M. (2009). Marrow stromal cell transplantation in stroke and traumatic brain injury. Neurosci. Lett. 456, 120–123.
47. Chopp, M. (2011). Orchestrating recovery: cell-based therapy for stroke. Transl. Stroke Res. 2, 241–242.
48. Zhang, J., and Chopp, M. (2013). Cell-based therapy for ischemic stroke. Exp. Opin. Biol. Ther. 13, 1229–1240.
49. Li, L., Chopp, M., Ding, G.L., Qu, C.S., Li, Q.J., Lu, M., Wang, S., Nejad–Davarani, S.P., Mahmood, A., and Jiang, Q. (2012). MRI measurement of angiogenesis and the therapeutic effect of acute marrow stromal cell administration on traumatic brain injury. J. Cereb. Blood Flow Metabolism 32, 2023–2032.
50. Li, L., Jiang, Q., Qu, C.S., Ding, G.L., Li, Q.J., Wang, S.Y., Lee, J.H., Lu, M., Mahmood, A., and Chopp, M. (2011). Transplantation of marrow stromal cells restores cerebral blood flow and reduces cerebral atrophy in rats with traumatic brain injury: in vivo MRI study. J. Neurotrauma 28, 535–545.
51. Arganda–Carreras, I, Kybicc, J., and Ortiz–de-Solorzanod, C. (2008). bUnwarpJ: consistent and elastic registration in ImageJ. Methods and Applications
52. Chen, J., Sanberg, P.R., Li, Y., Wang, L., Lu, M., Willing, A.E., Sanchez–Ramos, J., and Chopp, M. (2001). Intravenous administration of human umbilical cord blood reduces behavioral deficits after stroke in rats. Stroke 32, 2682–2688.
53. Li, L., Jiang, Q., Ding, G., Zhang, L., Zhang, Z.G., Li, Q., Panda, S., Kapke, A., Lu, M., Ewing, J.R., and Chopp, M. (2009). MRI identification of white matter reorganization enhanced by erythropoietin treatment in a rat model of focal ischemia. Stroke 40, 936–941.
54. van der Zijden, J.P., van der Toorn, A., van der Marel, K., and Dijkhuizen, R.M. (2008). Longitudinal in vivo MRI of alterations in perilesional tissue after transient ischemic stroke in rats. Exp. Neurol. 212, 207–212.
55. Schaechter, J.D., Fricker, Z.P., Perdue, K.L., Helmer, K.G., Vangel, M.G., Greve, D.N., and Makris, N. (2009). Microstructural status of ipsilesional and contralesional corticospinal tract correlates with motor skill in chronic stroke patients. Hum. Brain Mapp. 30, 3461–3474.
56. Kou, Z., and Iraji, A. (2014). Imaging brain plasticity after trauma. Neural Regen. Res. 9, 693–700.
57. Smith, J.M., Lunga, P., Story, D., Harris, N., Le Belle, J., James, M.F., Pickard, J.D., and Fawcett, J.W. (2007). Inosine promotes recovery of skilled motor function in a model of focal brain injury. Brain 130, 915–925.
58. Inglese, M., Makani, S., Johnson, G., Cohen, B.A., Silver, J.A., Gonen, O., and Grossman, R.I. (2005). Diffuse axonal injury in mild traumatic brain injury: a diffusion tensor imaging study. J. Neurosurg. 103, 298–303.
59. Long, J.A., Watts, L.T., Chemello, J., Huang, S., Shen, Q., and Duong, T.Q. (2015). Multiparametric and longitudinal MRI characterization of mild traumatic brain injury in rats. J. Neurotrauma 32, 598–607.
60. Wu, H., Mahmood, A., Qu, C., Xiong, Y., and Chopp, M. (2012). Simvastatin attenuates axonal injury after experimental traumatic brain injury and promotes neurite outgrowth of primary cortical neurons. Brain Res. 1486, 121–130.
61. Xiong, Y., Qu, C., Mahmood, A., Liu, Z., Ning, R., Li, Y., Kaplan, D.L., Schallert, T., and Chopp, M. (2009). Delayed transplantation of human marrow stromal cell-seeded scaffolds increases transcallosal neural fiber length, angiogenesis, and hippocampal neuronal survival and improves functional outcome after traumatic brain injury in rats. Brain Res. 1263, 183–191.
62. Mahmood, A., Lu, D. and Chopp, M. (2004). Marrow stromal cell transplantation after traumatic brain injury promotes cellular proliferation within the brain. Neurosurgery 55, 1185–1193.
63. Mahmood, A., Lu, D. and Chopp, M. (2004). Intravenous administration of marrow stromal cells (MSCs) increases the expression of growth factors in rat brain after traumatic brain injury. J. Neurotrauma 21, 33–39.
64. Shen, L.H., Li, Y., Gao, Q., Savant–Bhonsale, S., and Chopp, M. (2008). Down-regulation of neurocan expression in reactive astrocytes promotes axonal regeneration and facilitates the neurorestorative effects of bone marrow stromal cells in the ischemic rat brain. Glia 56, 1747–1754.
65. Shen, L.H., Li, Y., and Chopp, M. (2010). Astrocytic endogenous glial cell derived neurotrophic factor production is enhanced by bone marrow stromal cell transplantation in the ischemic boundary zone after stroke in adult rats. Glia 58, 1074–1081.
66. Morganti–Kossmann, M.C., Rancan, M., Stahel, P.F., and Kossmann, T. (2002). Inflammatory response in acute traumatic brain injury: a double-edged sword. Curr. Opin. Crit. Care 8, 101–105.
67. Iihoshi, S., Honmou, O., Houkin, K., Hashi, K., and Kocsis, J.D. (2004). A therapeutic window for intravenous administration of autologous bone marrow after cerebral ischemia in adult rats. Brain Res. 1007, 1–9.

Address correspondence to:
Quan Jiang, PhD
Department of Neurology
Henry Ford Hospital
B126, Education & Research Building
2799 West Grand Boulevard
Detroit, MI 48202

E-mail: QJIANG1@hfhs.org